Molecular Crystals and Liquid Crystals
Publication details, including instructions for authors and subscription information:
http://www.tandfonline.com/loi/gmcl20

Critical Reexamination of Berreman's Theory on Surface Anchoring

Jun-ichi Fukuda [a b], Makoto Yoneya [a b] & Hiroshi Yokoyama [a b]

[a] Nanotechnology Research Institute (NRI), National Institute of Advanced Industrial Science and Technology (AIST), Umezono, Tsukuba, Japan

[b] Liquid Crystal Nano-System Project, ERATO/SORST, Japan Science and Technology Agency (JST), Tokodai, Tsukuba, Japan

Version of record first published: 22 Feb 2010

To cite this article: Jun-ichi Fukuda, Makoto Yoneya & Hiroshi Yokoyama (2010): Critical Reexamination of Berreman's Theory on Surface Anchoring, Molecular Crystals and Liquid Crystals, 516:1, 12-25

To link to this article: http://dx.doi.org/10.1080/15421400903397058

Mol. Cryst. Liq. Cryst., Vol. 516: pp. 12–25, 2010

ISSN: 1542-1406 print/1563-5287 online
DOI: 10.1080/15421400903397058

Taylor & Francis
Taylor & Francis Group

Critical Reexamination of Berreman's Theory on Surface Anchoring

JUN-ICHI FUKUDA,[1,2] MAKOTO YONEYA,[1,2] AND HIROSHI YOKOYAMA[1,2]

[1]Nanotechnology Research Institute (NRI), National Institute of Advanced Industrial Science and Technology (AIST), Umezono, Tsukuba, Japan
[2]Liquid Crystal Nano-System Project, ERATO/SORST, Japan Science and Technology Agency (JST), Tokodai, Tsukuba, Japan

We critically reexamine well-known Berreman's theory [Phys. Rev. Lett. **28***, 1683 (1972)] on the anchoring of a nematic liquid crystal due to its elastic distortions induced by a sinusoidally grooved surface. We put emphasis on the effect of azimuthal distortions of the director* $\mathbf{n}$ *and the contribution of saddle-splay surface elasticity characterized by* K_{24}*. We give a correct calculation of the anchoring energy and show that Berreman's theory gives a correct result only when* $K_1 = K_2$ *and* $K_{24} = 0$*, where* K_1 *and* K_2 *are the splay and twist elastic constants, respectively. We also present our preliminary numerical attempts to evaluate the anchoring energy of a surface with square patterns and compare the anchoring energy calculated numerically with an analytical one obtained by a direct extension of our theoretical argument on one-dimensional parallel grooves.*

Keywords Berreman's theory; Frank elasticity; nematic liquid crystal; numerical calculation; surface anchoring; surface elasticity

I. Introduction

Surface anchoring of a liquid crystal has long been one of the major research subjects in the field of liquid crystals [1–3], mainly because of its relevance to various applications of liquid crystals that include flat displays. Achieving desirable surface anchoring properties are highly important in those applications and understanding the underlying mechanisms is crucial in the appropriate control of surface anchoring. Although inter-molecular interactions between liquid crystals and surface substrates (polymers in many cases) have been considered responsible for surface anchoring [4–6], a different mechanism, the elastic distortion of a liquid crystal due to its

This work is in part supported by Kakenhi (Grant-in-Aid for Scientific Research) on Priority Area "Soft Matter Physics" from the Ministry of Education, Culture, Sports, Science and Technology of Japan, and the Sasakawa Scientific Research Grant from the Japan Science Society.

Address correspondence to Jun-ichi Fukuda, Nanotechnology Research Institute, AIST, 1-1-1 Umezono, Tsukuba 305-8568, Japan. E-mail: fukuda.jun-ichi@aist.go.jp

contact with non-flat surfaces, has long been regarded as another important source of surface anchoring. For the past decade, interest in the latter mechanism has been growing because there have been increasing number of attempts, based on recent rapid progress in nanotechnology, to tailor microscopically grooved surfaces to realize various anchoring properties [7–16].

The first theoretical study on surface anchoring induced by the elastic distortions of a liquid crystal in contact with a non-flat surface was carried out by Berreman [17]. He considered a one-dimensional sinusoidally grooved surface that imposes local tangential anchoring and discussed how nematic liquid crystals are distorted above it. His work is simple enough and therefore seems to capture the essence of surface anchoring induced by non-flat surfaces. It has motivated numerous subsequent theoretical [18–21] as well as experimental [22–24] studies on the relation between anchoring properties and surface geometry.

In our previous work [25–27], however, we critically reexamined Berreman's theory of surface anchoring and argued that his seemingly reasonable assumption of no azimuthal rotation of the director $\boldsymbol{n}$ is in fact unjustifiable; it is in general incompatible with a boundary condition at the surface. We also noticed that saddle-splay surface elasticity (whose associated elastic constant is K_{24}) does play an important role [26]. In this paper we will first describe in Section II how to calculate the anchoring energy including the contribution of saddle-splay elasticity. We will discuss in detail what results from the presence of saddle-splay elasticity and compare our result from that of Berreman's theory. The following section, Section III will be devoted to a numerical verification of our analytical argument. Since numerical calculation of the anchoring energy a one-dimensional sinusoidally grooved surface has already been presented in a previous paper [28], here we will show our preliminary study on the anchoring of a surface with two-dimensional square pattern. Our analytical argument on one-dimensional grooves can be readily extended to surfaces with arbitrary patterns [27], and therefore direct comparison of our numerical results with theory is possible. Concluding remarks are given in Section IV.

II. Theoretical Argument

A. Calculation of the Anchoring Energy of One-Dimensional Sinusoidal Grooves

In this section, we present the details of the calculation of the elastic energy of a distorted nematic liquid crystal in contact with a sinusoidally grooved surface [25–27]. This elastic energy is nothing but the anchoring energy we want to obtain.

The average orientational order of a nematic liquid crystal is denoted by a unit vector $\boldsymbol{n}(\boldsymbol{r})$ referred to as director. The Frank energy, or the elastic energy due to non-uniform $\boldsymbol{n}$, is written as [1,29,30]

$$F = \frac{1}{2}\int dr\{K_1(\nabla\cdot\boldsymbol{n})^2 + K_2(\boldsymbol{n}\cdot\nabla\times\boldsymbol{n})^2 + K_3(\boldsymbol{n}\times\nabla\times\boldsymbol{n})^2 - K_s\nabla\cdot(\boldsymbol{n}\nabla\cdot\boldsymbol{n} + \boldsymbol{n}\times\nabla\times\boldsymbol{n})\}. \tag{1}$$

Here K_1, K_2, and K_3 are splay, twist, and bend elastic constants, respectively, which characterizes bulk deformation of $\boldsymbol{n}$. The last term in Eq. (1) is the saddle-splay elastic term, which is often referred to surface elastic term because it is converted

to surface integral and does not contribute to the bulk Euler-Lagrange equation as we shall see below. We have introduced the symbol

$$K_s \equiv K_2 + K_{24}, \tag{2}$$

where K_{24} is the saddle-splay elastic constant [29–31]. We notice that for the elastic energy F to be positive-definite,

$$K_3 \geq 0, \quad 0 \leq K_s \leq 2K_1, \quad K_s \leq 2K_2 \tag{3}$$

must be fulfilled [30,32]. Here we do not consider the splay-bend term $K_{13}\nabla\cdot(\boldsymbol{n}\nabla\cdot\boldsymbol{n})$, because this term renders the problem of finding the profile of $\boldsymbol{n}$ minimizing F ill-defined [29,33], and even the existence of this term has been questioned [34].

We assume uniform alignment of $\boldsymbol{n}$ along the x-direction infinitely away from the surface and that the distortion of $\boldsymbol{n}$ from the uniform alignment is small enough. Then $\boldsymbol{n}$ is written as $\boldsymbol{n}\simeq(1, n_y, n_z)$ with $|n_y|$ and $|n_z|$ being much smaller than unity. Then retaining only second-order terms in n_y and n_z is sufficient for the following discussion, allowing analytical calculation of the anchoring energy. The Frank energy (1) then becomes

$$\begin{aligned} F = \frac{1}{2}\int d\boldsymbol{r}(&K_1(\partial_y n_y + \partial_z n_z)^2 + K_2(\partial_y n_z - \partial_z n_y)^2 + K_3[(\partial_x n_y)^2 + (\partial_x n_z)^2] \\ &- 2K_s(\partial_y n_y \partial_z n_z - \partial_y n_z \partial_z n_y)). \end{aligned} \tag{4}$$

We consider the case where a surface with sinusoidal groove is in contact with a nematic liquid crystal. The height of the surface with respect to a reference plane, for which we take $z=0$, is assumed to be

$$\zeta(x,y) = A\sin(q(x\sin\phi + y\cos\phi)) \equiv A\sin(\boldsymbol{q}\cdot\boldsymbol{r}_\perp) \tag{5}$$

where A and q (>0) are the amplitude and the wavenumber of the surface undulations, and ϕ denotes the angle between $\boldsymbol{n}$ at infinity (x-direction) and the groove direction. We have introduced symbols $\boldsymbol{q}\equiv(q\sin\phi,\ q\cos\phi)$ and $\boldsymbol{r}_\perp\equiv(x,\ y)$. The geometry of our system is illustrated in Figure 1. The nematic liquid crystal is filled in a semi-infinite region $z>\zeta(x,\ y)$ and the assumption of small distortions of $\boldsymbol{n}$ requires $qA\ll 1$. We also assume planer degenerate anchoring at the grooved surface; i.e., the director $\boldsymbol{n}$ is always perpendicular to the surface normal $\boldsymbol{\nu}$, but there is no preferred direction as long as $\boldsymbol{n}\cdot\boldsymbol{\nu}=0$ is fulfilled. Since $\boldsymbol{\nu}\|(\partial\zeta/\partial x,\ \partial\zeta/\partial y,\ -1)$, the condition of planar degenerate anchoring at the surface is explicitly written as

$$\frac{\partial\zeta}{\partial x} + n_y\frac{\partial\zeta}{\partial y} - n_z = 0. \tag{6}$$

Equation (6) does not give any boundary condition for n_y because $n_y\partial\zeta/\partial y$ gives a contribution higher order in qA. The leading-order term in Eq. (6) yields a boundary condition for n_z which reads

$$n_z = \frac{\partial\zeta}{\partial x} = qA\sin\phi\cos(\boldsymbol{q}\cdot\boldsymbol{r}_\perp). \tag{7}$$

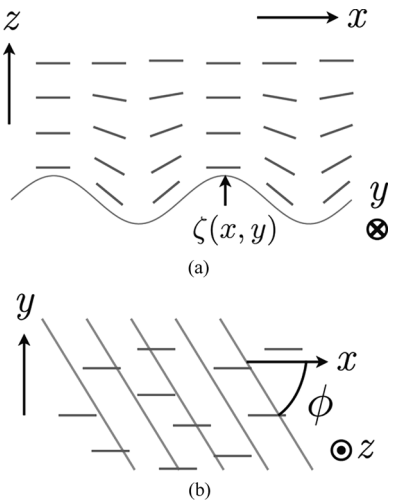

Figure 1. Illustrations of the geometry of the system. Short lines describe the direction of $\boldsymbol{n}$.

The full variational principle $\delta F = 0$ applied to the Frank elastic energy (4) results in a set of Euler-Lagrange equations in the bulk for n_y and n_z:

$$0 = -K_1\partial_y(\partial_y n_y + \partial_z n_z) + K_2\partial_z(\partial_y n_z - \partial_z n_y) - K_3\partial_x^2 n_y, \tag{8}$$

$$0 = -K_1\partial_z(\partial_y n_y + \partial_z n_z) - K_2\partial_y(\partial_y n_z - \partial_z n_y) - K_3\partial_x^2 n_z, \tag{9}$$

together with an additional condition at the surface that reads

$$\begin{aligned} 0 = &-K_1(\partial_y n_y + \partial_z n_z)\delta n_z + K_2(\partial_y n_z - \partial_z n_y)\delta n_y \\ &+ K_s(\partial_y n_y \delta n_z - \partial_y n_z \delta n_y) \end{aligned} \tag{10}$$

where δn_y and δn_z are the infinitesimal variations of the director at the surface. As noted above, the constant K_s characterizing the surface elasticity appears only in Eq. (10), not in Eqs. (8) and (9). The presence of the boundary condition for n_z, Eq. (7), implies $\delta n_z = 0$, which yields

$$-K_s\partial_y n_z + K_2(\partial_y n_z - \partial_z n_y) = 0. \tag{11}$$

To obtain the equilibrium director profile (n_y, n_z), we must solve the Euler-Lagrange Eqs. (8) and (9) under the boundary conditions at the surface (7) and (11), together with those at $z = +\infty$: $n_y = n_z = 0$. They can be solved analytically to give

$$n_z = qA\sin\phi\cos(\boldsymbol{q}\cdot\boldsymbol{r}_\perp)\left\{e^{-qzg_1(\phi)} + \frac{K_s}{K_3}\cot^2\phi\left(e^{-qzg_1(\phi)} - e^{-qzg_2(\phi)}\right)\right\}, \tag{12}$$

$$\begin{aligned} n_y = &\, qA\sin\phi\sin(\boldsymbol{q}\cdot\boldsymbol{r}_\perp) \\ &\times\left\{\frac{\cos\phi}{g_1(\phi)}e^{-qzg_1(\phi)} + \frac{K_s}{K_3}\cot^2\phi\left(\frac{\cos\phi}{g_1(\phi)}e^{-qzg_1(\phi)} - \frac{g_2(\phi)}{\cos\phi}e^{-qzg_2(\phi)}\right)\right\}, \end{aligned} \tag{13}$$

where we have defined $g_i(\phi) = \sqrt{\cos^2\phi + (K_3/K_i)\sin^2\phi}(i = 1, 2)$. We note that Eqs. (12) and (13) have already been obtained by Wolff *et al.* [35], although they did not discuss the explicit form of the anchoring energy as we shall give below.

Substitution of Eqs. (12) and (13) into Eq. (4) yields the elastic energy due to the distortion of the director induced by a grooved surface, which is the anchoring energy we intend to obtain. The resultant anchoring energy per unit surface area is

$$f(\phi) = \frac{1}{4}A^2q^3\frac{\sin^2\phi}{g_1(\phi)} \times \left\{K_3\sin^2\phi + K_s\cos^2\phi\left(2 - \frac{K_s}{K_3}\frac{g_1(\phi)g_2(\phi) - \cos^2\phi}{\sin^2\phi}\right)\right\}. \tag{14}$$

The former term of Eq. (14) gives the intrinsic contribution of the bulk elastic energy (K_1, K_2 and K_3) that has already been derived in our previous work [25]. The latter reflects the contribution from the saddle-splay elastic term ($K_s = K_2 + K_{24}$) [26]. In the following section, we will discuss in detail the difference between our result, Eq. (14), and that of Berreman [17], and consider how surface elastic term contributes to surface anchoring.

B. Discussion: Berreman's Assumption

We notice first that most of the assumptions employed in our theoretical argument are exactly the same as those in Berreman's; small distortions of $\boldsymbol{n}$ to use the second-order form of the elastic energy (Eq. (4)), and local planar degenerate anchoring resulting in Eq. (7).

An important assumption in Berreman's theory not used in ours is the absence of azimuthal distortion of $\boldsymbol{n}$, that is, $n_y = 0$ in our terminology. This assumption greatly simplifies the discussion because only one variable n_z has to be taken care of Berreman argued [17] that this assumption is justified when $K_1 = K_2$, because then Eq. (8) becomes independent of n_z and one can easily verify that $n_y = 0$ indeed satisfies Eq. (8). Conversely, however, Berreman's assumption of $n_y = 0$ becomes invalid when $K_1 \neq K_2$; since Eq. (8) is now a coupled equation of n_y and n_z, in general $n_y = 0$ cannot fulfill Eq. (8) unless $\partial_y\partial_z n_z = 0$ (note that $\partial_y\partial_z n_z = 0$ holds when $\sin\phi = 0$ or $\cos\phi = 0$; i.e., $\boldsymbol{n}$ is parallel or perpendicular to the grooves). Therefore Berreman's theory is invalid when $K_1 \neq K_2$. Detailed comparison between our result and Berreman's in the case of $K_1 = K_2$ will be presented in Section II.D.

We note also that when $n_y = 0$, the saddle-splay elastic energy becomes zero as can be easily seen from Eq. (4). Therefore by its nature Berreman's theory cannot deal with the contribution from the saddle-splay surface elasticity. We will return to the discussion on surface elasticity in Section II.E.

Finally we notice that Elgeti and Schmid [21] avoided the use of the assumption of $n_y = 0$ to derive the anchoring energy of a surface of general shape, although they did not include saddle-splay surface elasticity. Therefore their argument is almost the same as ours in Ref. [25]. and yields [36], when applied to one-dimensional grooves described by Eq. (5), the same anchoring energy as in Ref. [25].

C. Rapini-Papoular Anchoring Strength

It is often convenient for the discussion of anchoring properties to introduce the Rapini–Papoular [37] anchoring strength W defined by $f(\phi) \simeq (1/2)W(\phi - \phi_e)^2$ for $|\phi - \phi_e| << 1$, where ϕ_e denotes the direction of the easy axis and in the present case, $\phi_e = 0$. It is easily found that $W = \partial^2 f / \partial \phi^2|_{\phi=\phi_e}$, and thus from Eq. (14), we have

$$W = \frac{1}{2} A^2 q^3 K_s \left(2 - \frac{1}{2} K_s \frac{K_1 + K_2}{K_1 K_2} \right). \tag{15}$$

It is important to notice that this Rapini–Papoular anchoring strength comes solely from the latter term of Eq. (14), or the contribution from saddle-splay surface elasticity. Therefore, the presence of the anchoring of Rapini–Papoular type is a direct manifestation of non-zero saddle-splay surface elasticity. When the saddle-splay surface elastic term is absent, or $K_s = 0$, we recover $W = 0$, one of our main conclusions of Ref. [25]. One can readily find that W can be zero also when

$$K_s = 4K_1 K_2 / (K_1 + K_2), \tag{16}$$

and careful analysis using the inequalities (3) reveals that Eq. (16) is fulfilled if and only if $K_1 = K_2 = K_s/2$. On the other hand, we can easily find also that

$$K_s = 2K_1 K_2 / (K_1 + K_2) \tag{17}$$

gives the maximum W for fixed K_1 and K_2. It is also shown from Eq. (3) that W cannot be negative.

D. Comparison with Berreman's Result for $K_1 = K_2$

As noted in Section II.B, Berreman assumed $n_y = 0$ in his calculation of the anchoring energy, arguing that it could be justified when $K_1 = K_2$. In this subsection we concentrate on the case with $K_1 = K_2$ and we will denote these elastic constants as K, i.e., $K = K_1 = K_2$. In Berreman's theory one just has to solve Eq. (9) for a single variable n_z under the boundary conditions, Eq. (7) and $n_z = 0$ at $z = +\infty$. The solution reads

$$n_z = qA \sin\phi \cos(\boldsymbol{q} \cdot \boldsymbol{r}_\perp) \exp\left(- \frac{qz}{\sqrt{\cos^2\phi + \frac{K_3}{K} \sin^2\phi}} \right), \tag{18}$$

and the resultant anchoring energy is

$$f_{\text{Berreman}}(\phi) = \frac{1}{4} K A^2 q^3 \sin^2\phi \sqrt{\cos^2\phi + \frac{K_3}{K} \sin^2\phi}. \tag{19}$$

On the other hand, our anchoring energy (14) in the case of $K_1 = K_2 = K$ becomes

$$f(\phi) = \frac{1}{4} A^2 q^3 \frac{\sin^2\phi}{\sqrt{\cos^2\phi + \frac{K_3}{K} \sin^2\phi}} \left\{ K_3 \sin^2\phi + K_s \left(2 - \frac{K_s}{K} \right) \cos^2\phi \right\}. \tag{20}$$

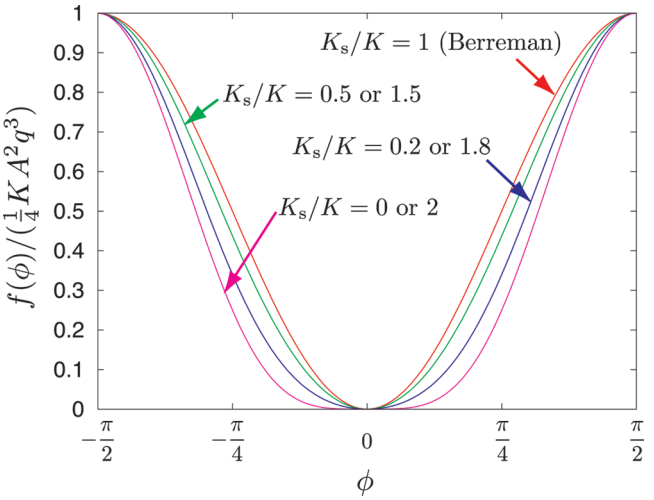

Figure 2. Plot of the anchoring energy f for various K_s. Here $K_1 = K_2 = K_3 = K$ has been assumed.

Comparing Eq. (19) with Eq. (20), we find that $f_{\text{Berreman}}(\phi) = f(\phi)$ for arbitrary ϕ if and only if $K = K_s$, or $K_{24} = 0$.

This finding can be understood in a different and simpler manner; $n_z \neq 0$ and $n_y = 0$ satisfy the boundary condition (7) for arbitrary ϕ only when $K_s = K_2 (= K)$. One can also verify from Eq. (13) that $n_y \equiv 0$ when $K_s = K_1 = K_2 (= K)$.

It is important to note that the inequality

$$f(\phi) \leq f_{\text{Berreman}}(\phi) \tag{21}$$

is always satisfied, because $K_s = K$, which yields $f(\phi) = f_{\text{Berreman}}(\phi)$, gives the maximum of $f(\phi)$ with respect to the variation of K_s (see Eq. (20)). Equation (21) clearly indicates that Berreman's director profile with $n_y = 0$ does not give the minimum Frank energy in general, which reflects that fact that Berreman's profile does not satisfy the boundary condition (7) and therefore is not consistent with the full variational principle $\delta F = 0$. In Figure 2 we plot $f(\phi)$ for various K_s in a further simplified case of $K_1 = K_2 = K_3 = K$. It can be easily seen from Figure 2 that Eq. (21) is always satisfied. The invariance of $f(\pi/2)$ with the variation of K_s can be easily understood from Eq. (20). It is also seen from Figure 2 that the anchoring strength W discussed in Section II.C, which corresponds to the curvature of $f(\phi)$ at $\phi = 0$, sensitively depends on K_s. In an extreme case of $K_s/K = 0$ or 2, $f(\phi)$ around $\phi = 0$ is almost flat, reflecting $W = 0$. In that case, $f(\phi) \propto \sin^4\phi$ as argued in Ref. [25], which marks a sharp contrast with $f_{\text{Berreman}}(\phi)$ proportional to $\sin^2\phi$ (see Eq. (19)).

E. Contribution of Surface Elasticity

Here we discuss how surface elasticity contributes to surface anchoring energy in a more quantitative manner. For clarity, in this subsection we assume $K_1 = K_2 = K_3 = K$. From our results, the contributions to the anchoring energy from splay, twist, bend, and saddle-splay elasticity are written, respectively, as

$$f_1 = \frac{1}{8} KA^2 q^3 \sin^2\phi \left(\sin^2\phi + \frac{K_s}{K} \cos^2\phi \right)^2, \tag{22}$$

$$f_2 = \frac{1}{8} KA^2 q^3 \sin^2\phi \cos^2\phi \left(\frac{K_s}{K} \right)^2, \tag{23}$$

$$f_3 = \frac{1}{8} KA^2 q^3 \sin^4\phi \left(1 + \cos^2\phi \left(1 - \frac{K_s}{K} \right)^2 \right), \tag{24}$$

$$f_s = \frac{1}{2} KA^2 q^3 \frac{K_s}{K} \left(1 - \frac{K_s}{K} \right) \sin^2\phi \cos^2\phi. \tag{25}$$

We notice first that the twist energy (23) becomes zero in the absence of surface elasticity ($K_s = 0$), as has already been argued in Ref. [25]. The splay and the twist energies, Eqs. (22) and (23), are monotonically increasing function of K_s, while the bend energy (24) is minimized when $K_s/K = 1$. The maximum of surface elastic energy (25) alone is located at $K_s/K = 1/2$, not at $K_s/K = 1$.

We note that the contributions from the bulk elastic energies sum up to

$$f_1 + f_2 + f_3 = \frac{1}{4} KA^2 q^3 \sin^2\phi \left(\sin^2\phi + \left(\frac{K_s}{K} \right)^2 \cos^2\phi \right), \tag{26}$$

which is again a monotonically increasing function of K_s, in spite of the minimization of f_3 at $K_s/K = 1$. Therefore, the increase in the bulk elastic energy with the increase of K_s, although distributed to splay, twist and bend in a non-trivial manner as seen in Eqs. (22)–(24), is compensated by the decrease of the surface elastic energy f_s for $K_s > 1/2$, resulting in the maximum of the total anchoring energy at $K_s/K = 1$.

In Section II.B we have noted that Berreman's assumption of $n_y = 0$ yields zero surface elastic energy, which can be seen also from Eq. (25); we have shown in the previous section that Berreman's theory corresponds to choosing $K_s = K$. It should be emphasized that zero f_s in Berreman's theoretical treatment does not imply that the surface elastic term is absent ($K_s = 0$) in his theory.

III. Numerical Argument

In this section, we will give our numerical attempts to evaluate the anchoring energy of a grooved surface. Numerical calculations of the anchoring energy of one-dimensionally grooved surfaces whose theoretical form was discussed in the previous section were already carried out in our previous paper [28]. Therefore in this paper we will present our preliminary studies on the anchoring of surfaces with square patterns. Before showing our numerical results, we will briefly review how our theoretical argument presented above can be extended to surfaces with square patterns [27].

A. Theory on Anchoring of a Surface with Square Pattern

In this section we consider a surface whose height $\zeta(x, y)$ with respect to the reference plane $z = 0$ is written as

$$\begin{aligned}\zeta(x,y) &= A\{\sin(q(x\sin\phi + y\cos\phi)) + \sin(q(x\sin(\phi+\pi/2) + y\cos(\phi+\pi/2)))\} \\ &= A\{\sin(q(x\sin\phi + y\cos\phi)) + \sin(q(x\cos\phi - y\sin\phi))\}\end{aligned} \tag{27}$$

This profile is just the superposition of a set of sinusoidal parallel grooves and the other set of sinusoidal grooves perpendicular to the former. We note that here again the director at infinity ($z \to \infty$) is along the x-direction. In our previous study [27], we showed that the total anchoring energy of a grooved surface whose height can be written as a Fourier series becomes the sum of the contributions from each Fourier component. Therefore the analytical anchoring energy of the present surface is given by

$$f_{\mathrm{sq}}(\phi) = f(\phi) + f(\phi + \pi/2), \tag{28}$$

in which $f(\phi)$ is the anchoring energy of a one-dimensionally grooved surface whose explicit form is found in Eq. (14). In the following subsection, we will calculate the anchoring energy numerically for a surface with its profile written as Eq. (27) and compare it with Eq. (28) to find out the validity of Eq. (28) for small qA, and what happens when qA cannot be regarded as small enough.

B. Numerical Calculation of the Anchoring Energy

The details of the numerical calculation is given in our previous work [28], and elsewhere [39]. Thus we will mention the essential part of the numerical calculation. Instead of the geometry described in the previous subsection, we consider a surface whose height with respect to $z = 0$ is $h(x, y) = A(\sin qx + \sin qy)$, and fix the director at $z = L_z$ to $\boldsymbol{n} = (\cos\phi, \sin\phi, 0)$. This geometry is equivalent to that in the previous subsection except that L_z is finite here. Our numerical system is then described as $0 \le x < 2\pi/q$, $0 \le y < 2\pi/q$ and $h(x, y) \le z \le L_z$, with periodic boundary conditions along the x and y directions. After introducing a variable ξ satisfying $z = \xi + (1 - \xi/L_z)h(x, y)$, our system can be mapped onto a rectangular solid in the (x, y, ξ) space. We discretize our system in the (x, y, ξ) space by $N \times N \times (N+1)$ grid points with equal spacings: $\Delta x = \Delta y = 2\pi/qN$ and $\Delta\xi = L_z/N$. In the present calculation, we choose $N = 32$ and $L_z = 2\pi/q$ (or $\Delta\xi = \Delta x, \Delta y$).

We calculate numerically for various ϕ the profile of $\boldsymbol{n}$ that minimizes the original Frank elastic energy (1) (not the quadratic form (4)), with a fixed boundary condition at $z = \xi = L_z$ as described above, and a planar degenerate boundary condition at $z = h(x, y)$ or $\xi = 0$. The latter implies that $\boldsymbol{n}$ at the surface can point to any direction so long as it is perpendicular to the local surface normal.

We note that since we deal with a finite system, spontaneous twist deformations exist in the bulk. On the other hand, in our theoretical argument above, twist deformation is absent at $z \to \infty$, because the presence of finite twist in the bulk is, however small it is, incompatible with the fixed boundary condition of $\boldsymbol{n}$ at infinity.

Evaluation of the twist in the bulk and corresponding azimuthal angle of the director $\phi(0)$ at the grooved surface is carried out using the procedure described in Ref. [28]. Then from the total Frank elastic energy calculated numerically, we subtract the contribution from the twist deformations in the bulk, which results in the anchoring energy $f_a(\phi(0))$ that we want to obtain.

For material parameters, we choose, as in our previous study [28], $K_1/K_3 = 0.7$, $K_2/K_3 = 0.5$ and $K_s/K_3 = 0.6$ or 1. Our choice of K_1/K_3 and K_2/K_3 is consistent with the inequality $K_3 > K_1 > K_2$ fulfilled in most of the rodlike liquid crystals. $K_s/K_3 = 0.6$ satisfies the equality $K_s = (K_1 + K_2)/2$ derived by Nehring and Saupe [31] from their molecular theory, although previous experiments do not necessarily support its validity [38]. $K_s/K_3 = 1$ is the largest value allowed by Ericksen's inequality (3).

In Figure 3, we plot the rescaled anchoring energy $(f_a(\phi(0)) - f_a(45°))/\left(\frac{1}{4}K_3A^2q^3\right)$ as a function of the azimuthal angle at the grooved surface $\phi(0)$ for $qA = \pi/160 \simeq 0.020$. Notice from the symmetry of a square pattern that we have to show only the results for $0° \le \phi(0) \le 45°$. The solid lines represent the analytical results deduced from Eq. (28). We find a perfect agreement between theory and numerical calculations, which clearly indicates the validity of our theoretical results as well as that of our numerical scheme for the calculation of the anchoring energy.

Next we show in Figure 4 the calculated results for $qA = \pi/16 \simeq 0.20$. Again the agreement between theory and numerical calculations is quite good. Notice that in our theoretical argument we assumed $|qA| \ll 1$, and we cannot safely say that $qA \simeq 0.20$ is much smaller than unity. This result indicates that the range of qA in which a theoretical result is valid is larger than expected from the original assumption of $|qA| \ll 1$.

Figure 5 presents the results for larger surface height, $qA = 3\pi/16 \simeq 0.59$. Now deviations between theory and numerical calculations are clearly observed.

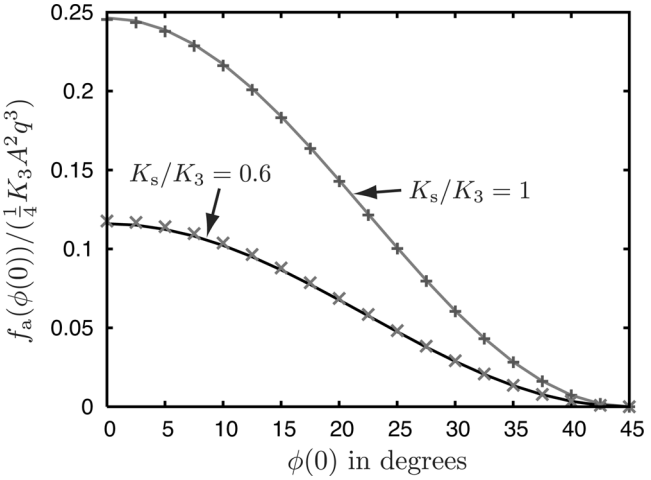

Figure 3. Plot of the numerically calculated anchoring energy f_a as a function of the azimuthal angle of the director at the grooved surface, $\phi(0)$ for $qA = \pi/160 \simeq 0.020$. Solid lines represent analytical results.

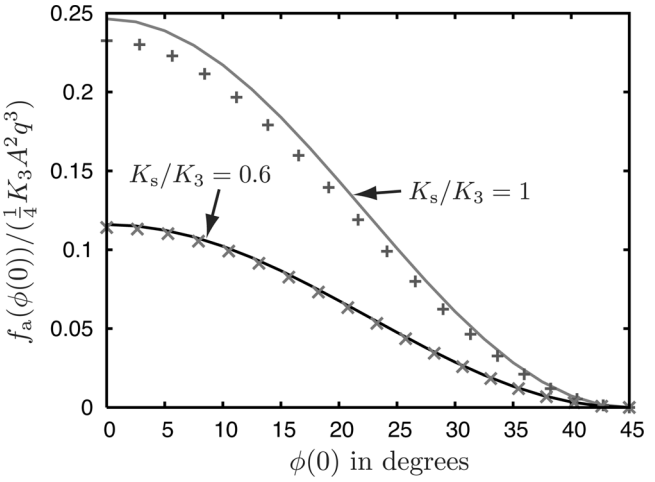

Figure 4. The same as Fig. 3 for $qA = \pi/16 \simeq 0.20$.

Nevertheless, qualitative feature of the analytical result that the minimum of $f_a(\phi(0))$ is located at $\phi(0) = 45^\circ$ is maintained in the numerical results. We also find that the numerical results for $K_s/K_3 = 0.6$ give better agreement with theory than those for $K_s/K_3 = 1$. This tendency was observed also in the case of one-dimensional parallel grooves [28], and we attributed it to the fact that the overall profile of the azimuthal angle of the director ***n*** resembles that naively expected from theory more closely for $K_s/K_3 = 0.6$ [28]. In the case of $K_s/K_3 = 1$, distribution of the azimuthal angle is wider than that in the case of $K_s/K_3 = 0.6$, which results in an inevitable deviation of the director profile from the one expected theoretically. We speculate that the above reasoning holds also for the present case of a surface with square patterns. Detailed analysis will be given elsewhere [39].

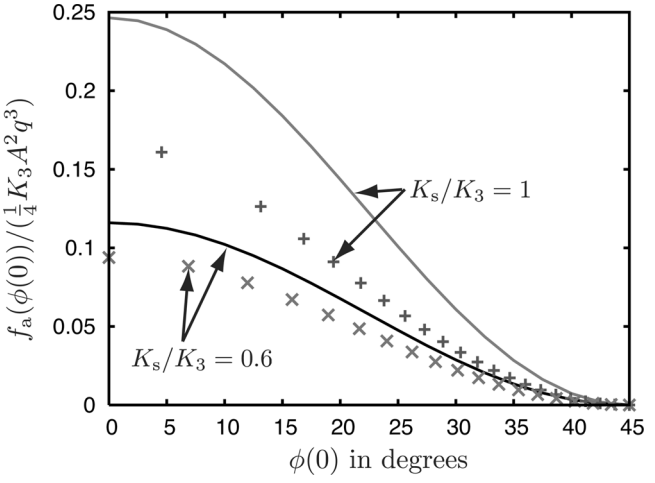

Figure 5. The same as Fig. 3 for $qA = 3\pi/16 \simeq 0.59$.

IV. Conclusion

In the first part of this paper, we have critically reexamined a well-known theory of Berreman on the surface anchoring of a nematic liquid crystal due to its elastic distortions induced by a non-flat surface. His assumption of no azimuthal distortion of the director ($n_y = 0$ in our terminology) cannot be justified; $n_y = 0$ cannot be a solution of the Euler-Lagrange equations in the bulk in the case $K_1 \neq K_2$, and even when it is in the case of $K_1 = K_2$, $n_y = 0$ cannot in general satisfy the boundary condition at the surface derived from variational principle.

Furthermore, we have discussed the effect of saddle-splay surface elastic term, i.e., $-(K_s/2)\nabla \cdot (\boldsymbol{n}\nabla \cdot \boldsymbol{n} + \boldsymbol{n} \times \nabla \times \boldsymbol{n})$ with $K_s = K_2 + K_{24}$. We have shown that this surface elastic term does play a decisive role in the anchoring energy of a one-dimensionally grooved surface and that Berreman's theory by its nature cannot deal with surface elasticity properly because of the assumption of $n_y = 0$. One of our important conclusions is that non-zero anchoring strength W in the Rapini-Papoular sense is a direct manifestation of non-zero saddle-splay surface elasticity; in its absence ($K_s = 0$), W becomes zero. We have also made a careful comparison of our results with Berreman's to find that Berreman's theory gives a correct result only when $K_1 = K_2 = K_s$ (or $K_{24} = 0$). Almost all of the experimental studies concerning liquid crystal anchoring induced by surface geometry based the interpretations of their results on Berreman's theory to some extent. Moreover, many of previous theoretical attempts to extend Berreman's theory did not pay attention to the validity of his assumption ($n_y = 0$), and surface elasticity. Therefore those previous experimental and theoretical studies may have to be critically reinterpreted or reexamined.

Since non-zero Rapini-Papoular anchoring strength reflects the presence of surface elasticity as noted above, direct information on the saddle-splay surface elastic constant may be deduced from careful measurements of the Rapini-Papoular anchoring strength of a sinusoidally grooved surface. We notice here that Nehring and Saupe [31] derived a relation $K_{24} = (K_1 - K_2)/2$ or $K_s = (K_1 + K_2)/2$ from their molecular theory. This relation together with $K_1 = K_2$ happens to yield Berreman's result. Yokoyama [34] argued, however, that this Nehring-Saupe relation should be replaced by an inequality $K_{24} \geq (K_1 - K_2)/2$. Moreover, previous experimental measurements of K_{24} [38] have shown that some nematic liquid crystals can have almost the largest K_{24} that is consistent with the inequality (3). From Eq. (15) or (17), W becomes smaller for larger K_{24} as long as $K_{24} \geq K_2(K_1 - K_2)/(K_1 + K_2)$. Therefore, very small Rapini-Papoular anchoring strength may be achieved by choosing materials with large K_{24}.

In the second part, we have presented our numerical attempts to evaluate the anchoring energy of a grooved surface. We have considered a surface with square patterns whose height with respect to a reference plane $z = 0$ is given by $h(x, y) = A(\sin qx + \sin qy)$. When $|qA| \lesssim 0.2$, the azimuthal-angle dependence of numerically calculated anchoring energy is in excellent agreement with that of the anchoring energy evaluated analytically, which demonstrates the wide range of validity of the analytical argument in spite of its assumption of $|qA| \ll 1$, together with the integrity of our numerical calculation. In the case of $|qA| \simeq 0.6$, the difference between calculated and analytical anchoring energies crucially depends on surface elastic constant, again indicating the important role of surface elasticity in surface anchoring. We believe that numerical calculation as well as analytical argument will be a promising tool for the investigation of liquid crystal anchoring induced by surface geometry.

References

[1] de Gennes, P. G. & Prost, J. (1993). *The Physics of Liquid Crystals*, 2nd ed. Oxford University Press: Oxford.
[2] Castellano, J. A. (1983). *Mol. Cryst. Liq. Cryst.*, *94*, 33.
[3] Yokoyama, H. (1997). In: *Handbook of Liquid Crystal Research*, Collings, P. J. & Patel, J. S. (Eds.), Oxford University Press: Oxford, Chap. 6.
[4] Cheng, J. & Boyd, G. D. (1979). *Appl. Phys. Lett.*, *35*, 444.
[5] Geary, J. M., Goodby, J. W., Kmetz, A. R. & Patel, J. S. (1987). *J. Appl. Phys.*, *62*, 4100.
[6] Ishihara, S., Wakemoto, H., Nakazima, K., & Matsuo, Y. (1989). *Liq. Cryst.*, *4*, 669.
[7] Rüetschi, M., Grütter, P., Fünfschilling, J., & Güntherodt, H.-J. (1994). *Science*, *265*, 512.
[8] Wood, E. L., Bradberry, G. W., Cann, P. S., & Sambles, J. R. (1997). *J. Appl. Phys.*, *82*, 2483.
[9] (a) Wen, B., Mahajan, M. P., & Rosenblatt, C. (2000). *Appl. Phys. Lett.*, *76*, 1240; (b) Wen, B. & Rosenblatt, C. (2001). *J. Appl. Phys.*, *89*, 4747.
[10] (a) Kim, J.-H., Yoneya, M., Yamamoto, J., & Yokoyama, H. (2001). *Appl. Phys. Lett.*, *78*, 3055; (b) Kim, J.-H., Yoneya, M., & Yokoyama, H. (2002). *Nature (London)*, *420*, 159.
[11] Zhang, B., Lee, F. K., Tsui, O. K. C., & Sheng, P. (2003). *Phys. Rev. Lett.*, *91*, 215501.
[12] Lee, F. K., Zhang, B., Sheng, P., Kwok, H. S. & Tsui, O. K. C. (2004). *Appl. Phys. Lett.*, *85*, 5556.
[13] Honma, M., Yamamoto, K., & Nose, T. (2004). *J. Appl. Phys.*, *96*, 5415.
[14] Varghese, S., Crawford, G. P., Bastiaansen, C. W. M., de Boer, D. K. G., & Broer, D. (2005). *J. Appl. Phys. Lett.*, *86*, 181914.
[15] (a) Gwag, J. S., Yoneya, M. & Yokoyama, H. (2006). IDW '06 (Otsu, Japan, Dec.), LCT7-4 L; (b) Gwag, J. S., Fukuda, J., Yoneya, M., & Yokoyama, H. (2007). *Appl. Phys. Lett.*, *91*, 073504; (c) Gwag, J. S., Oh-e, M., Yoneya, M., Yokoyama, H., Satou, H., & Itami, S. (2007). *J. Appl. Phys.*, *102*, 063501; (d) Gwag, J. S., Kim, J. H., Yoneya, M., & Yokoyama, H. (2008). *Appl. Phys. Lett.*, *92*, 153110.
[16] (a) Yeung, F. S. & Kwok, H. S. (2006). *Appl. Phys. Lett.*, *88*, 063505; (b) Yeung, F. S., Ho, J. Y., Li, Y. W., Xie, F. C., Tsui, O. K., Sheng, P., & Kwok, H. S. (2006). *Appl. Phys. Lett.*, *88*, 051910.
[17] Berreman, D. W. (1972). *Phys. Rev. Lett.*, *28*, 1683; (1973). *Mol. Cryst. Liq. Cryst*, *23*, 215; See also Ref. [1], p. 115.
[18] Faetti, S. (1987). *Phys. Rev. A*, *36*, 408.
[19] Bryan-Brown, G. P., Towler, M. J., Bancroft, M. S. & McDonnell, D. G. (1994). Proceedings of International Display Research Conference (Society for Information Display, California) 209.
[20] Fournier, J.-B. & Galatola, P. (1999). *Phys. Rev. E*, *60*, 2404.
[21] Elgeti, J. & Schmid, F. (2005). *Eur. Phys. J. E*, *18*, 407.
[22] Lee, E. S., Better, P., Miyashita, T., Uchida, T., Kano, M., Abe, M., & Sugawara, K. (1993). *Jpn. J. Appl. Phys. Part 2.*, *32*, L1436.
[23] Newsome, C. J., O'Neill, M., Farley, R. J., & Bryan-Brown, G. P. (1998). *Appl. Phys. Lett.*, *72*, 2078.
[24] Barberi, R., Dozov, I., Giocondo, M., Iovane, M., Martinot-Lagarde, Ph., Stoenescu, D., Tonchev, S., & Tsonev, L. V. (1998). *Eur. Phys. J. B*, *6*, 83.
[25] Fukuda, J., Yoneya, M., & Yokoyama, H. (2007). *Phys. Rev. Lett.*, *98*, 187803.
[26] Fukuda, J., Yoneya, M., & Yokoyama, H. (2007). *Phys. Rev. Lett.*, *99*, 139902(E).
[27] Fukuda, J., Gwag, J. S., Yoneya, M., & Yokoyama, H. (2008). *Phys. Rev. E*, *77*, 011702.
[28] Fukuda, J., Yoneya, M. & Yokoyama, H. (2008). *Phys. Rev. E*, *77*, 030701(R).
[29] Chandrasekhar, S. (1992). *Liquid Crystals*, 2nd ed. Cambridge University Press.
[30] Virga, E. G. (1994). *Variational Theories for Liquid Crystals*, Chapman and Hall: London.

[31] Nehring, J. & Saupe, A. (1971). *J. Chem. Phys.*, *54*, 337.
[32] Ericksen, J. L. (1966). *Phys. Fluids*, *9*, 1205.
[33] Oldano, C. & Barbero, G. (1985). *Phys. Lett.*, *110A*, 213; (1985). *J. Phys. (Paris)*, *46*, 451.
[34] Yokoyama, H. (1997). *Phys. Rev. E*, *55*, 2938.
[35] Wolff, U., Greubel, W., & Krüger, H. (1973). *Mol. Cryst. Liq. Cryst.*, *23*, 187.
[36] Elgeti, J. (private communication).
[37] Rapini, A. & Papoular, M. (1969). *J. Phys. (Paris), Colloq.*, *30*, C4–54.
[38] Crawford, C. P. (2001). In: "*Physical Properties of Liquid Crystals: Nematics*" Dunmer, D. A., Fukuda, A., & Luckhurst, G. R. INSPEC. The Institution of Electrical Engineers: London.
[39] Fukuda, J., Yoneya, M., & Yokoyama, H. (2009). *Phys. Rev. E.*, *79*, 011705.